Tropical stratospheric upwelling impacts the tropical equilibrium climate sensitivity by reducing the effective forcing

Diego Jiménez-de-la-Cuesta,[a] and Hauke Schmidt[a]

[a] *Max-Planck-Institut für Meteorologie, Hamburg, Deutschland*

ABSTRACT: An atmospheric composition feedback mechanism modulates the global equilibrium climate sensitivity (ECS) through changes in the tropical upper-tropospheric and lower-stratospheric (UTLS) water vapor (Dietmüller et al. 2014; Muthers et al. 2014; Nowack et al. 2015; Marsh et al. 2016; Nowack et al. 2018; Chiodo and Polvani 2019). The feedback mechanism is caused by the acceleration of the Brewer-Dobson circulation (BDC, e.g. Butchart 2014). This process changes the ozone (O_3) concentration, resulting in a drier and cooler UTLS region than without O_3 changes. Thus, the planetary long-wave emissivity increases, and the ECS decreases. However, the BDC alone already provides dynamical cooling through the tropical stratospheric upwelling, potentially impacting the ECS. Here, we analyze the implications of this effect from a tropical clear-sky perspective, applying a one-dimensional radiative-convective equilibrium (RCE) model that explicitly accounts for the adiabatic cooling by the BDC and includes an interactive representation of O_3. We study how increasing upwelling modifies the change of the tropical energy budget resulting from a doubling of CO_2. An increase in upwelling reduces the tropical ECS mainly through an increased tropical energy export related to the adiabatic cooling. The atmospheric composition feedback through O_3 contributes less than 30% to the tropical ECS reduction. Due to the dominance of the energy export, any impact on the global ECS will depend on the redistribution of the energy in the extratropics. We show that GCMs simulate similar changes of the tropical energy export under increased upwelling which corroborates that the findings obtained with the RCE approach bear relevance for the global climate.

1. Introduction

There is a broad scientific consensus that in response to tropospheric warming under CO_2 forcing, the tropical tropopause layer (TTL) rises and warms, and the meridional Brewer-Dobson circulation (BDC, Brewer 1949; Dobson 1956) accelerates (Butchart 2014). This includes an accelerated upwelling in the tropical lower stratosphere, which pushes O_3-poor air upwards and reduces the O_3 concentration in the tropical upper troposphere and lower stratosphere (UTLS), leading to a relative cooling and drying of this region. Several modeling studies identified that this connection between temperature, circulation, and composition provides a radiative feedback mechanism that modulates Earth's equilibrium climate sensitivity (ECS, Dietmüller et al. 2014; Muthers et al. 2014; Nowack et al. 2015; Marsh et al. 2016; Nowack et al. 2018; Chiodo and Polvani 2019). A drier UTLS would lead to higher planetary emissivity and, hence, a reduced ECS (Nowack et al. 2015; Dacie et al. 2019). The magnitude of this reduction is, however, debated. This effect has received attention because in many present-day climate models used for instance in the experiments for the Coupled Model Intercomparison project (CMIP, Taylor et al. 2012; Eyring et al. 2016) the O_3 concentration is still prescribed and this feedback ignored.

Corresponding author: Diego Jiménez-de-la-Cuesta, diego.jimenez@mpimet.mpg.de

Upwelling in the tropical lower stratosphere influences the temperature and, in consequence, the humidity in this region also directly through adiabatic cooling. This effect should provide a feedback on surface temperatures and hence influence ECS. The effect has received less attention, so far, probably because it is implicitly included in CMIP-type climate models. However, as the magnitude of upwelling acceleration as simulated in models differs (e.g., Yoshida et al. 2018), it is of interest to understand its impact. Here we study, how such circulation changes influence ECS, to what extent this effect is caused by changes in forcing or feedback, and how it compares to changes caused by the atmospheric composition feedback.

The BDC acceleration increases the tropical UTLS cooling. The energy exported from the tropical UTLS should warm the extratropical lower stratosphere. Here, we only study the effect of circulation change on the tropical ECS under clear-sky conditions. We leave for future studies the question of how the extratropical stratospheric warming modifies the regional radiative feedback mechanisms and thereby changes global ECS. We use the radiative-convective equilibrium (RCE) framework, commonly applied for representing the tropical atmosphere. Specifically, we choose the one-dimensional RCE model `konrad` (Kluft et al. 2019) in an extended configuration that includes the adiabatic cooling of the tropical stratospheric upwelling. Dacie et al. (2019) used this configuration to study how changes of the O_3 profile affect TTL temperature, humidity, and the tropical ECS under prescribed, constant tropical stratospheric upwelling. We now study

how changes in the tropical stratospheric upwelling due to warming can modulate the tropical ECS. The analysis focuses on the effects of the dynamical cooling changes on the energy budget in terms of tropical forcing and feedback. Initially, we fix O_3 to isolate the direct, adiabatic effect of the upwelling, and then analyze the combined adiabatic and diabatic effects. We also test the sensitivity of the circulation effects to the specifics of the relative humidity profile. Finally, we show that the magnitude of upwelling increase affects tropical climate energy export and feedbacks also in CMIP models.

2. Methodology

a. The RCE framework

In a first-order approximation, the tropical troposphere is in radiative-convective equilibrium: the temperature profile is mainly determined by a balance between radiative cooling and moist-convective warming. This framework in its one-dimensional version should describe the mean behavior of the tropical troposphere (Ramanathan and Coakley 1978). Early climate studies have used the one-dimensional framework, e.g., in the seminal papers by Manabe and Strickler (1964) and Manabe and Wetherald (1967), to understand the thermal structure of the atmosphere and its response to forcing. In the era of complex global climate models, this simple framework is still relevant for understanding processes that the complexity of state-of-the-art models would otherwise obscure (e.g., Birner and Charlesworth 2017; Kluft et al. 2019; Dacie et al. 2019; Bourdin et al. 2021; Bao, Jiawei and Stevens, Bjorn and Kluft, Lukas and Jiménez-de-la-Cuesta, Diego 2021).

b. Overview of `konrad` *configuration*

The one-dimensional RCE model `konrad` has two main components: a radiative transfer model (RRTMG) and a convective adjustment. The model calculates a temperature profile resulting from the diabatic temperature tendencies from the radiative transfer scheme. The energy is then vertically redistributed so that the temperature profile follows a moist-adiabatic temperature lapse rate. This adjustment simulates the effect of convection, ergo the name convective adjustment. Under clear-sky conditions, we use in all experiments a hard convective adjustment (Dacie et al. 2019) that sharply separates the tropospheric region in RCE from the region in purely radiative equilibrium above it. Concentrations of radiatively active gases, other than H_2O, CO_2 and O_3, are prescribed constant as in Kluft et al. (2019) and Dacie et al. (2019). The CO_2 concentration is vertically-uniform and doubled for the climate change experiments. In most of our experiments, the relative humidity (RH) is set to a vertically-uniform profile of 0.4 in the troposphere. The stratospheric humidity is set by the specific humidity at the cold point. Additionally, we test the sensitivity of the results to the tropospheric RH profile. In those sensitivity experiments, we use another uniform and two more realistic C-shaped profiles (Bourdin et al. 2021), presented in Table 1. The C-shaped profiles are temperature dependent in the sense that they are not prescribed in height coordinates but in temperature coordinates. Therefore, changes in the temperature profile will lead to changes in the RH profile.

	RH / 1		
Name	Lower	Middle	Upper
U4	0.4	0.4	0.4
CB	0.8	0.3	0.6
U7	0.7	0.7	0.7
C8	0.8	0.4	0.8

TABLE 1. Characteristic relative humidity values of the vertical profiles used in the numerical experiments. The C-shaped profiles are functions of the temperature. Therefore, the values for the lower, middle, and upper troposphere are only indications. They are not constant over time but depend on the changes in the temperature profile.

Additional features of the `konrad` configuration used in this study are (a) the scheme representing the dynamical cooling provided by the BDC and (b) an interactive O_3 scheme. By definition, any pure RCE framework ignores the adiabatic cooling K of tropical stratospheric upwelling. We include it using the parameterization proposed by Birner and Charlesworth (2017),

$$K = -w \left[(\partial_z T) + \frac{g}{c_p} \right], \tag{1}$$

where w is a prescribed upwelling speed, g the gravitational acceleration, and c_p the specific heat of dry air at constant pressure. Via the temperature lapse rate $\partial_z T$, this cooling term can interact with diabatic processes, in particular atmospheric composition changes. K is set to zero below the convective top. The cooling term represents the BDC-driven energy transfer from the tropical UTLS region to the extratropical stratosphere. As this term is balanced in the extratropics, it acts in `konrad` as an energy sink (Dacie et al. 2019).

To calculate the O_3 profile, we use the linearized scheme proposed by Cariolle and Teyssèdre (2007) (hereafter called "Cariolle scheme"). It is a faster alternative to full chemistry models (see, e.g., Meraner et al. 2020). The linearization coefficients were calculated using a two-dimensional photochemical model, depending on latitude and height. The coefficients represent the dependencies of production-loss rates on the O_3 mixing ratio itself, temperature, and the overhead O_3 column. In `konrad`, we

use a tropical mean of these coefficients. O_3 and stratospheric upwelling can be coupled by using the prescribed upwelling speed to represent vertical transport of O_3. We use the scheme first to obtain an adequate O_3 reference profile that is then fixed for analyzing the direct (adiabatic) effects of upwelling changes. Secondly, the scheme is used interactively to study the combined adiabatic and diabatic effects, when O_3 responds to upwelling changes.

We use a 500-level vertical grid from 1000 hPa to 0.01 hPa in which the levels are evenly-spaced in $\ln p$ and provide a sufficient resolution in the TTL region (Kluft et al. 2019). All the experiments use a slab ocean with a thermal capacity equivalent to 1 m of water, a long-wave emissivity of 1, and a surface albedo of 0.2. In terms of the time control, we use a varying time stepping, with a maximum time step of 2 hours. All the simulations are run for 10 years, long enough to reach the steady state, given the small thermal capacity of our ocean.

c. Simulation strategy

As it is typical for studying ECS, we run experiments where the CO_2 concentration is doubled instantaneously, labeled `2xCO2`. These experiments start from a reference state obtained from the equilibrium state of a control experiment, labeled `control`. The `control` experiment has a prescribed reference upwelling speed $w^c = 0.2\,\mathrm{mm\,s^{-1}}$ which provides a relatively realistic reference O_3 profile (compare, e.g., with profiles presented in Meraner et al. 2020). Additionally, w^c is in the range of values estimated for the annually-averaged mean upwelling in the tropical (30° S to 30° N) lower stratosphere (e.g., Abalos et al. 2015). The equilibrium surface temperature is $T^*_{s,e} \approx 295\,\mathrm{K}$. The `2xCO2` experiments start from the `control` reference state and run until equilibrium. In each `2xCO2` experiment, we change the upwelling speed from the original w^c to values in the range of $0.0\,\mathrm{mm\,s^{-1}}$ to $0.4\,\mathrm{mm\,s^{-1}}$. However, only increases in upwelling speed are consistent with the expected changes in BDC and actual observations (e.g. Fu et al. 2019). For evaluating the direct effect of the upwelling changes on ECS, we prescribe the same O_3 profile for the `2xCO2` runs used in the `control` run.

The changes in upwelling due to the BDC acceleration are simulated in two ways: (a) by switching to the new upwelling speed instantaneously and, (b) providing a relationship between the surface warming and the upwelling. The CMIP ensemble suggests that such relationship is monotonically increasing. Therefore, we assume a simplified linear relationship

$$w_m(T_s) = w^c + m(T_s - T^*_{s,e}), \tag{2}$$

where $m > 0$ is the rate in which the upwelling changes with surface warming. Method (b) is more realistic than method (a). However, method (a) is more simple to understand. Afterwards, we incorporate the effects of a varying upwelling with surface warming to complete the picture.

To estimate the indirect effect of circulation on ECS that occurs via the atmospheric composition feedback we run additional `2xCO2` experiments in which O_3 is not prescribed but interactively calculated using the Cariolle scheme. Furthermore, we test the potential sensitivity of the results to the RH profiles listed in Table 1. Table 2 summarizes the experiments.

Experiment set	w / mm s^{-1}	O_3	RH
`control`	0.2	C	U4
			CB
			U7
			C8
`2xCO2`	0.0 – 0.4	P	U4
		C	
		P	CB
		C	
		P	U7
		C	
		P	C8
		C	
	$w_m(T_s)$	P	U4
		C	

TABLE 2. Main characteristics of the simulations. In the O_3 column, C indicates use of the Cariolle scheme and P prescribed O_3. The RH column provides the RH profile used for each set. In the column for w, experiments with $w_m(T_s)$ use equation (2) for several values of m.

3. Theory

a. The classical linearized forcing-feedback framework

The net global TOA radiative flux φ, the energy absorbed by the system, is related to the surface temperature T_s. If some forcing agent changes φ, T_s will adjust to balance the change. This relationship can be displayed in an NT-diagram, where the change of the TOA net radiative flux, $N(t) = \varphi(t) - \varphi^*_e$, is plotted versus the surface temperature change, $\Delta T_s(t) = T_s(t) - T^*_{s,e}$. φ^*_e and $T^*_{s,e}$ are the TOA flux and surface temperature of the equilibrium `control` state, respectively. Time dependencies are omitted in the following to simplify the notation. In an idealized global NT-diagram, the relationship is quasi-linear if we exclude the short starting curvature from the stratospheric temperature adjustment. The quasi-linearity justifies the classical linearized model $N \approx \hat{F} + \lambda \Delta T_s$ (Gregory et al. 2004), where the slope λ is the net radiative feedback parameter, and the y-intercept $\hat{F}$ is the effective radiative forcing. The surface temperature changes until the new equilibrium is

reached, i.e. when $\varphi = \varphi_e^*$ or, equivalently, $N \equiv 0$. This temperature change $\mathcal{S}$ is the ECS of the system. With this definition, $\hat{F} = -\lambda\mathcal{S}$, and we can write

$$N \approx \lambda(\Delta T_s - \mathcal{S}). \tag{3}$$

The net feedback parameter λ can hence be obtained from fitting the data points for the relationship between φ and ΔT_s.

b. The extended linearized forcing-feedback framework

In striking difference to a classical NT-diagram, our extended RCE framework has a changing energy sink introduced by the cooling rate (1). As mentioned above, the upwelling speed and changes in the temperature lapse-rate, modify the energy sink. Therefore, the forcing-feedback framework needs to be extended to account for this varying energy sink. If the tropics export more energy than in the `control` experiment, then the equilibrium net TOA radiative flux of the `2xCO2` experiment will be greater than that of the `control`: $\varphi_e > \varphi_e^*$. Conversely, if the tropics export less energy than in the `control`, $\varphi_e < \varphi_e^*$, and the equilibrium net TOA radiative flux of the `2xCO2` experiment will be smaller than in the `control`. Such behavior is present in the `2xCO2` experiments (Figure 1) where we change the upwelling speed instantaneously: the new equilibrium is not anymore reached at the zero line. Therefore, at equilibrium, $N = N_e = \varphi_e - \varphi_e^* \neq 0$. The quasi-linear behavior remains and $N_e = \hat{F} + \lambda\mathcal{S}$. So we define $F = \hat{F} - N_e$ as the tropical effective forcing in relation to the tropical net TOA radiative flux at the new equilibrium, whereas $\hat{F}$ is the tropical effective radiative forcing relative to the tropical net TOA radiative flux at the `control` equilibrium state. In the case of F, we do not speak of *radiative* forcing anymore because the energy export to the extratropics is not radiative in nature. Since N_e is the difference in the tropical TOA radiative flux between equilibrium states, it should represent the change in the tropical energy export arising from the upwelling speed change modifying the cooling rate (1). By definition, $F = -\lambda\mathcal{S}$ (Figure 1). This leads to an extension of equation (3):

$$N - N_e \approx \lambda(\Delta T_s - \mathcal{S}). \tag{4}$$

Using equation (4) on the data shown in Figure 1, we obtain λ, whereas $\mathcal{S}$ and N_e are known from the final equilibrium state. The gray dashed lines in Figure 1 are the result of the fitting process.

This extended framework is needed because the tropics are an open system when lateral energy export to the extratropics is considered and energy is not only redistributed within the system. The direct effect of N_e is, hence, an additional forcing of the system. One could integrate this direct effect in the feedback, but then the net tropical feedback

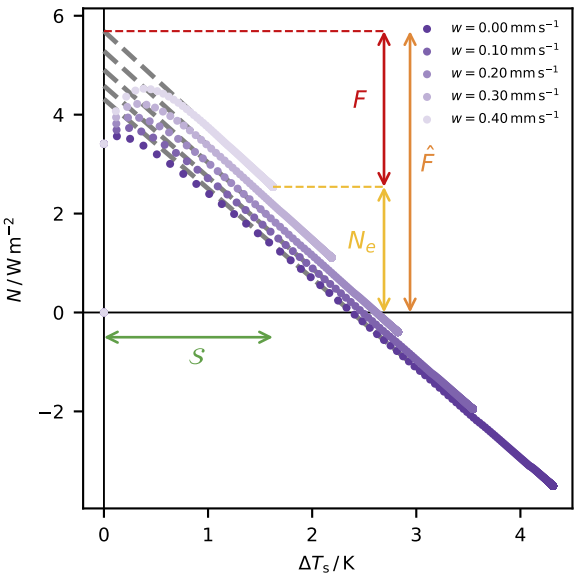

FIG. 1. NT-diagrams for the `2xCO2` experiments with prescribed O_3. Each shade of purple corresponds to an upwelling speed w. Lighter shades indicate increasing upwelling speed. The grey dashed lines correspond to the linear approximation of the N-ΔT_s relationship. With increasing tropical upwelling, $\mathcal{S}$ (green) is reduced, but the tropics equilibrate at a non-zero N. This is the change in tropical energy export N_e (yellow). Because of that, the forcing to which the tropics respond has the magnitude F (red), instead of $\hat{F}$ (orange).

λ would not be purely radiative. To keep the interpretation close to the classical forcing-feedback framework, we decided to consider the direct effect of N_e as an addition to the tropical effective radiative forcing $\hat{F}$, providing the not purely radiative F. The radiative feedback can change in response to the atmospheric temperature changes produced by the energy export as we will see in the results. However, these changes are less important than the direct effect. This is even true when the upwelling changes are implemented as a response to surface temperature changes via Equation (2).

4. Results

a. The `2xCO2` runs with prescribed O_3 and instantaneous changes in upwelling speed

The tropical ECS decreases with increasing upwelling speed, even though $\hat{F}$ increases (Figure 1). This is because with increasing upwelling speed, also the tropical energy export N_e increases, sustaining a new equilibrium at a higher net TOA radiative balance and a lower effective forcing F relative to the new equilibrium (Figure 2, upper left and right panels).

The change in tropical energy export appears as a linear function of w, consistent with the cooling term (1) that is proportional to the upwelling speed (Figure 2, upper left

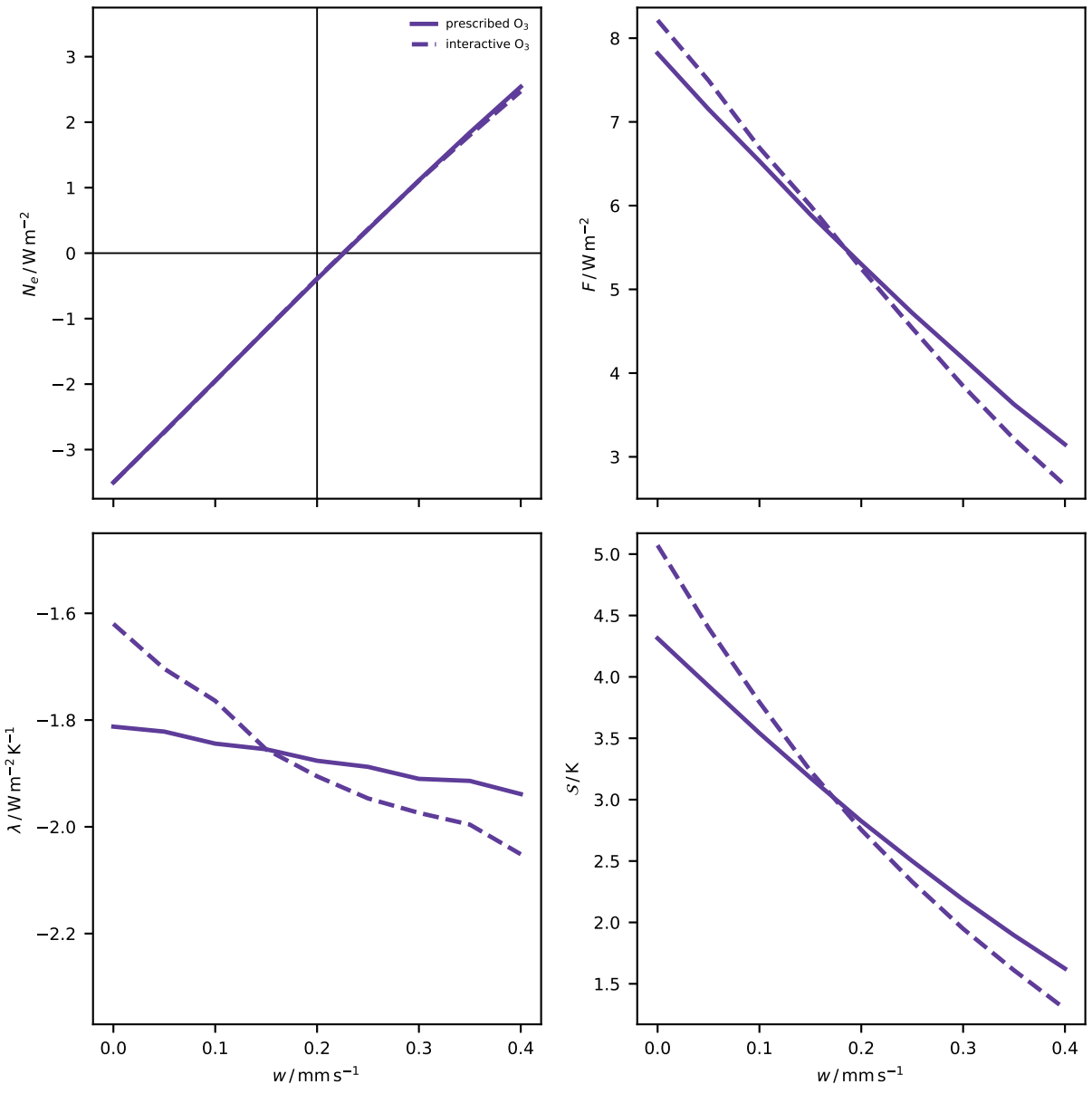

FIG. 2. Changes in the energy budget as a function of w. Continuous line: `2xCO2` experiments with prescribed O_3. Dashed line: `2xCO2` experiments with Cariolle O_3. Upper left panel: tropical energy export N_e. Upper right panel: Tropical effective forcing F. Lower left panel: tropical net radiative feedback parameter λ. Lower right panel: tropical equilibrium climate sensitivity $\mathcal{S}$.

panel). The change in the tropical energy export is not zero at w^c, a feature also explained by the cooling term: the increase in CO_2 changes the temperature lapse rate, in particular through stratospheric cooling, and reduces the energy export. In contrast, the change in the net radiative feedback parameter λ is small (Figure 2, lower left panel). The summary of the forcing and feedback contributions is the relationship between $\mathcal{S}$ and w (Figure 2, lower right panel). This relationship is slightly non-linear due to the slightly more negative λ for larger upwelling, but the reduction in $\mathcal{S}$ is mostly explained by the decreasing F.

A colder TTL with increasing upwelling initially reduces the outgoing long-wave radiation (OLR) and causes a larger $\hat{F}$. However, the finally dominating effect is the change in the N_e, which buffers the forcing, reducing F and $\mathcal{S}$ with increasing upwelling speed. The tiny strengthening of λ is a consequence of the drier atmosphere with increasing upwelling speed (Figure 3).

It may come as a surprise that the dominant effect of the increasing upwelling is the reduction of OLR, i.e. comes from its change of the lapse rate. The cooling from the upwelling also leads to a reduction of specific humidity which would increase the planetary emissivity and not reduce it. In the case of cooling from the upward shift of O_3 this latter effect is usually used to explain the reduction of ECS through the O_3 feedback as mentioned above, and which is also occuring in our experiment with interactive O_3 (see below). We think that the exact altitude of the cooling decides on which effect dominates. As it is implemented, the cooling from the O_3 shift affects the TTL, and thereby water vapor, more strongly than the adiabatic cooling of increased upwelling.

In summary, with increasing upwelling speed, the increased adiabatic cooling leads to stronger $\hat{F}$ but increases the tropical energy export, transferring part of the energy to the extratropics, reducing F and, therefore, $\mathcal{S}$. The associated drying of the atmosphere minimally strengthens λ.

b. The `2xCO2` runs with prescribed O_3 and evolving upwelling speed coupled to surface warming

In the real atmosphere, the upwelling can be expected to increase gradually with surface warming. We represent this by using expression (2). This gradual cooling reduces the lapse-rate feedback and thereby OLR over time, leading to a less negative λ (Figure 4). In Figure 5, we illustrate the case of $m = 0.05\,\mathrm{mm\,s^{-1}\,K^{-1}}$, in which equilibrium is reached at an upwelling speed $w_e \approx 0.307\,\mathrm{mm\,s^{-1}}$. The final change in the tropical energy export should be equal to the change observed in an experiment with an instantaneous change from $0.2\,\mathrm{mm\,s^{-1}}$ to w_e (Figures 4 and 5). Due to the gradual TTL cooling, the OLR is not strongly reduced at inception, as in the case of an instantaneous change in upwelling, ergo $\hat{F}$ is smaller. Because the equilibrium tropical energy export is the same as for an instantaneous change to $w = w_e$, also F has to be smaller (compare Figures 2 and 4). The decreases in λ and F balance exactly, such that $\mathcal{S}$ is equal in the experiments with evolving upwelling and the corresponding instantaneous change to $w = w_e$.

c. The `2xCO2` runs with Cariolle O_3 and instantaneous changes in upwelling speed

The simulations with interactive O_3 enable us to estimate the effect of the atmospheric composition feedback on ECS in comparison to the direct adiabatic effects of increased upwelling discussed above. However, we first evaluate the performance of the Cariolle scheme in `konrad` under CO_2 doubling. Table 3 lists the O_3 concentrations at 50 hPa and 30 hPa simulated by three GCMs with interactive chemistry (Dietmüller et al. 2014; Nowack et al. 2018; Marsh et al. 2016) as shown by Dacie et al. (2019). For comparison, we show a selection of `2xCO2` `konrad` simulations, with upwelling speeds from $0.2\,\mathrm{mm\,s^{-1}}$ (no change) to $0.4\,\mathrm{mm\,s^{-1}}$. The mixing ratios from the `control` experiment are near the ranges of the GCMs' `pi-Control` experiments. This confirms the usefulness of the Cariolle-approach in this simplified one-dimensional setting in accordance with Meraner et al. (2020) who discussed its usefulness in GCMs. We assume that the O_3 changes in the `abrupt-4xCO2` experiments with GCMs can be scaled for comparison with the `2xCO2` experiments by halving them. Changes in the mixing ratios for an upwelling increase to $0.3\,\mathrm{mm\,s^{-1}}$ fit best to the GCM simulations, whereas the $0.2\,\mathrm{mm\,s^{-1}}$ and $0.4\,\mathrm{mm\,s^{-1}}$ experiments under- and overestimate the O_3 reductions, respectively. A comparison of the O_3 profiles from the `control` and `2xCO2` simulations with upwelling speeds of $0.2\,\mathrm{mm\,s^{-1}}$ (Figure 3, lower right panel) shows that the effects from only temperature and photochemistry on O_3 are about an order of magnitude smaller than effects from upwelling changes of $0.1\,\mathrm{mm\,s^{-1}}$.

An increase in upwelling pushes the O_3 profile upwards (Figure 3, lower right) and enhances cooling in the TTL region mostly due to less absorption of short-wave radiation. This slightly changes the relationship of upwelling change with the tropical energy export, because of slightly different lapse rate compared to the case of prescribed O_3. It also leads to a considerably lower F, not so much because of a change in the energy export to the extratropics, but because of the reduced greenhouse effect from less water vapor which dominates the decrease of OLR from the lapse rate effect. In addition, the net feedback parameter λ depends more strongly on the upwelling change and is substantially more negative with increasing upwelling speed. This is likely due to the dependence of both water vapor and O_3 feedbacks on the upwelling velocity. Both, the weaker forcing and the stronger feedback contribute to stronger reductions of $\mathcal{S}$ with increasing upwelling speed in comparison to experiments with prescribed O_3 (Figure 2), where the change in forcing was the main factor for reducing $\mathcal{S}$. However, the larger part of the reduction of $\mathcal{S}$ with increasing upwelling comes from the adiabatic cooling: for an increase of $0.4\,\mathrm{mm\,s^{-1}}$, interactive O_3 chemistry only contributes 28% to the reduction of $\mathcal{S}$. The stronger non-linearity in $\mathcal{S}$ as a function of w now comes from the stronger change in λ with w.

d. The `2xCO2` runs with Cariolle O_3 and evolving upwelling speed coupled to surface warming

When introducing a gradual increase of upwelling together with Cariolle O_3, the relationship of the tropical energy export N_e with increasing w_e is almost identical to the case of fixed O_3, and both cases are identical to those with instantaneous upwelling changes. However, the weaker lapse-rate feedback introduced by the evolving

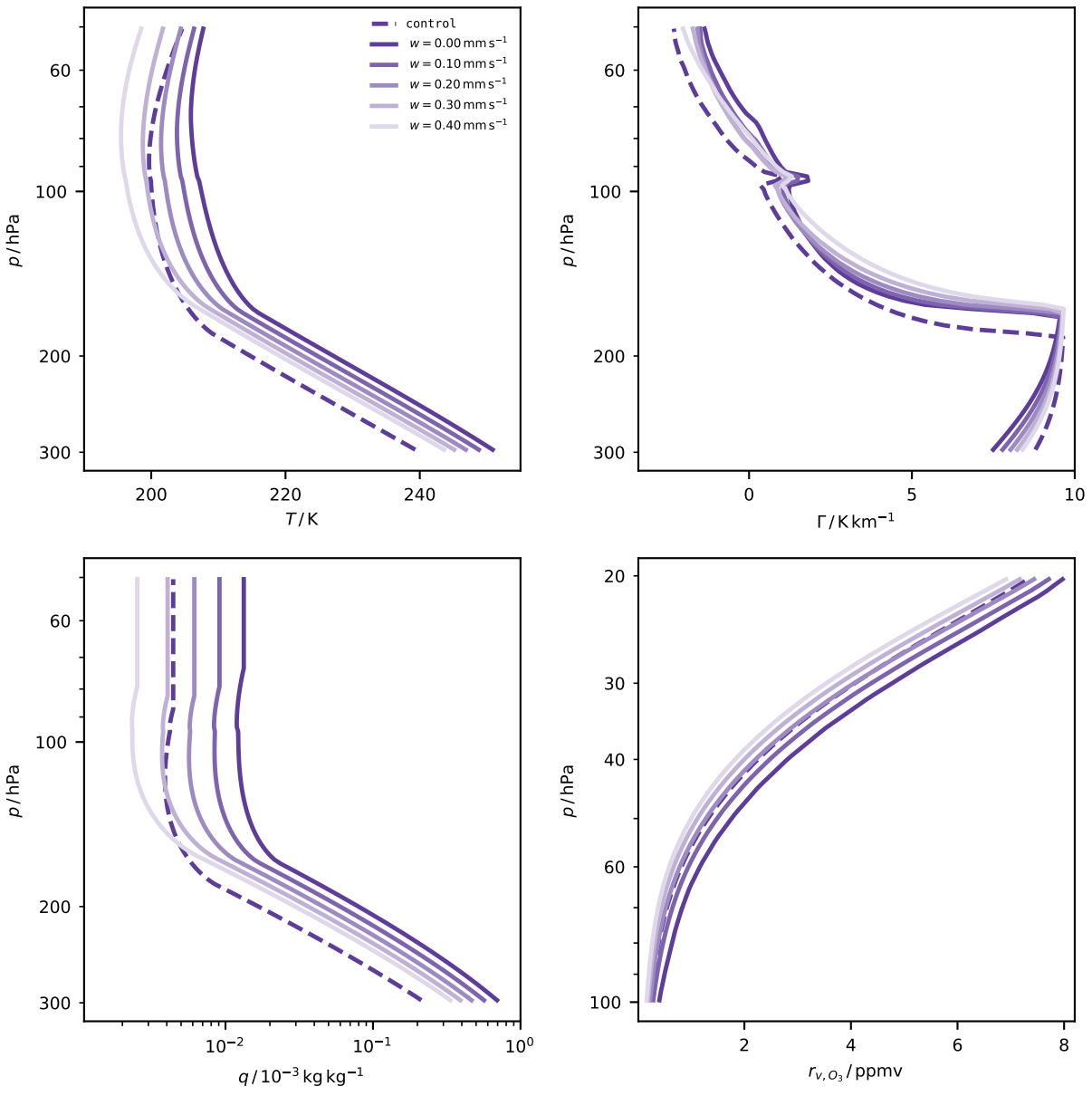

FIG. 3. Equilibrium tropical temperature T, lapse rate Γ, and specific humidity q for experiments with prescribed O_3 and instantaneous changes in upwelling speed. The O_3 volume mixing ratio r_{v,O_3} is shown for the Cariolle O_3 experiments. The `control` profile is the profile used for the prescribed O_3 experiments. Dashed lines: `control` experiment. Continuous lines: `2xCO2` experiments. Lighter shades of purple denote increasing upwelling speed.

upwelling in the prescribed O_3 experiments is now overcompensated by the weaker water-vapor feedback due to the joint effect of the atmospheric composition feedback and the upwelling cooling, resulting in a substantially negative net feedback λ, which again demonstrates the different consequences of the coolings directly caused by the upwelling and indirectly by the O_3 shift. As expected, $\mathcal{S}$ is again independent of the upwelling changing gradually or instantaneously, requiring that F does not reduce with w_e as strongly in the gradual as in the instantaneous case. (Figure 4).

e. The role of relative humidity

Bourdin et al. (2021) found that the tropical ECS is affected by the vertical distribution of RH. To identify if our results depend on the choice of the RH profile, we run

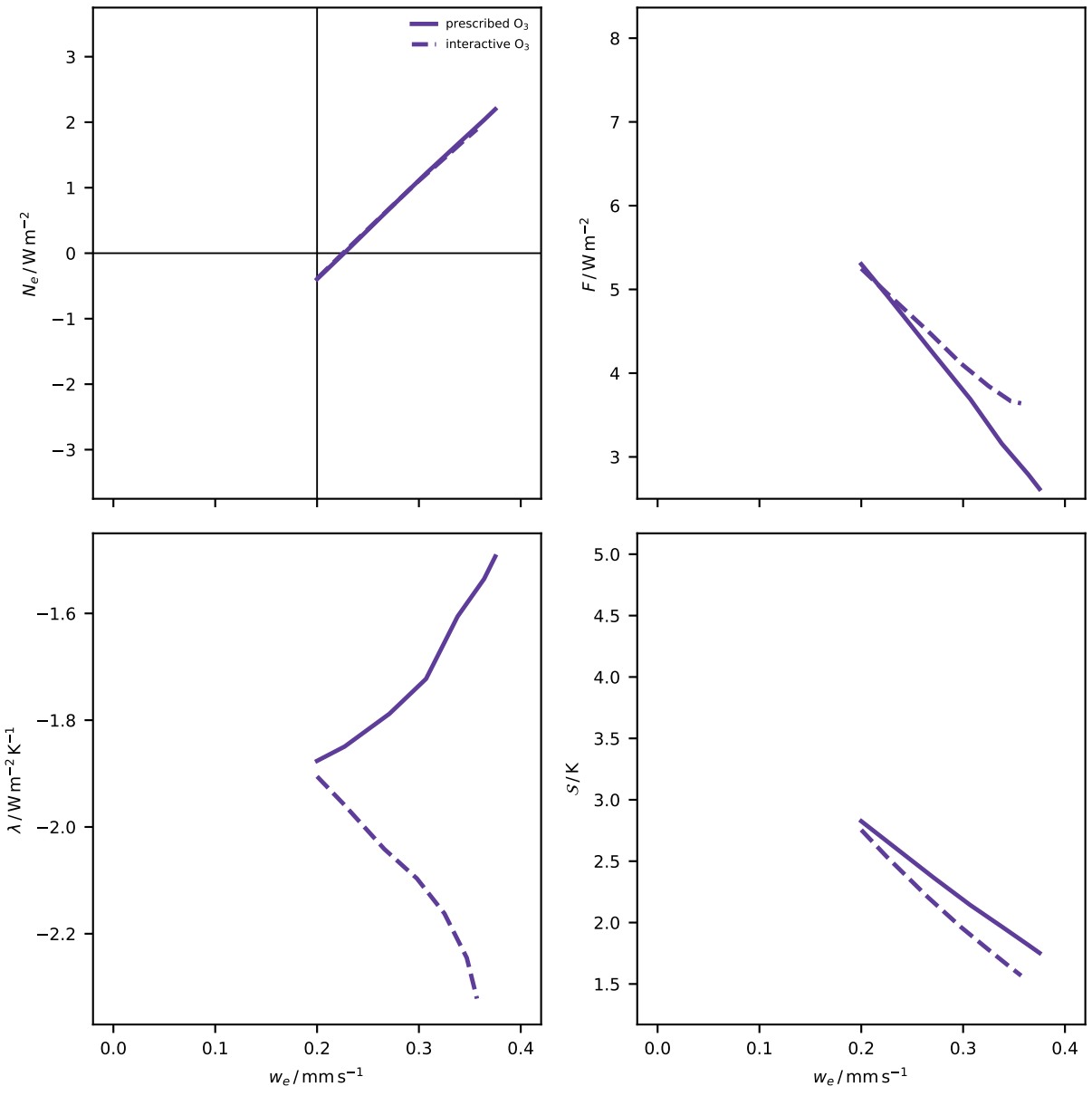

FIG. 4. Changes in the energy budget as a function of w_e for evolving upwelling. Continuous line: `2xCO2` experiments with prescribed O_3. Dashed line: `2xCO2` experiments with Cariolle O_3. Upper left panel: tropical energy export N_e. Upper right panel: Tropical effective forcing F. Lower left panel: tropical net radiative feedback parameter λ. Lower right panel: tropical equilibrium climate sensitivity $\mathcal{S}$. Shown only for m in the range $0.01\,\mathrm{mm\,s^{-1}\,K^{-1}}$ to $0.10\,\mathrm{mm\,s^{-1}\,K^{-1}}$

a complete set of experiments, analogous to the `control` and `2xCO2` experiments but for the three additional RH profiles from Table 1. Essentially, the relation of $\mathcal{S}$ with w is very similar for all RH profiles, but with a stronger non-linearity and a shift to higher values of $\mathcal{S}$ for more humid climates (Figure 6). We conclude that the main results presented above do not depend critically on the RH profile. According to Bourdin et al. (2021), however, higher RH values in the upper troposphere lead to higher $\mathcal{S}$. Thus, we would have expected a stronger difference between the results with the U4 and CB profiles. In our case, the shift to higher $\mathcal{S}$ values is more related to the middle tropospheric humidity. The shift is then likely the consequence of a narrower atmospheric window in the limit of the very humid climate U7.

Experiment	O_3 concentration / ppmv			
	30 hPa		50 hPa	
	nxCO2	control	nxCO2	control
Dietmüller et al. (2014)	−0.5	5.0	−0.6	1.5
Nowack et al. (2015)	−0.6	4.5	−0.5	1.8
Marsh et al. (2016)	−0.5	3.9	−0.3	1.3
2xCO2 $w = 0.200$	−0.02	3.92	−0.04	1.29
2xCO2 $w_e = 0.298$	−0.28		−0.19	
2xCO2 $w = 0.300$	−0.29		−0.19	
2xCO2 $w_e = 0.357$	−0.43		−0.26	
2xCO2 $w = 0.400$	−0.53		−0.31	

TABLE 3. Comparison with the O_3 concentration GCMs with interactive chemistry. The first three are GCM experiments: the abrupt-4xCO2 experiments. The two pairs of columns show the concentration at 50 hPa and 30 hPa for the climate change and the control experiments, respectively.

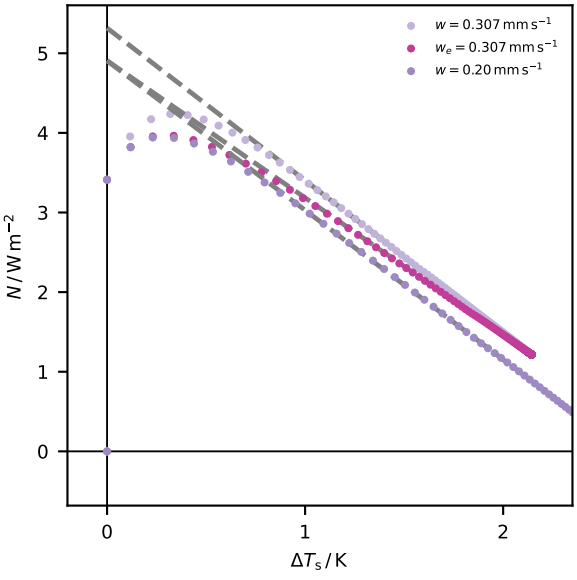

FIG. 5. NT-diagram for the 2xCO2 experiments with prescribed O_3 and varying upwelling. Shades of purple indicate the experiments with an instantaneous change in w, dark magenta the experiment using $w_m(T_s)$ with $m = 0.05\,\mathrm{mm\,s^{-1}\,K^{-1}}$.

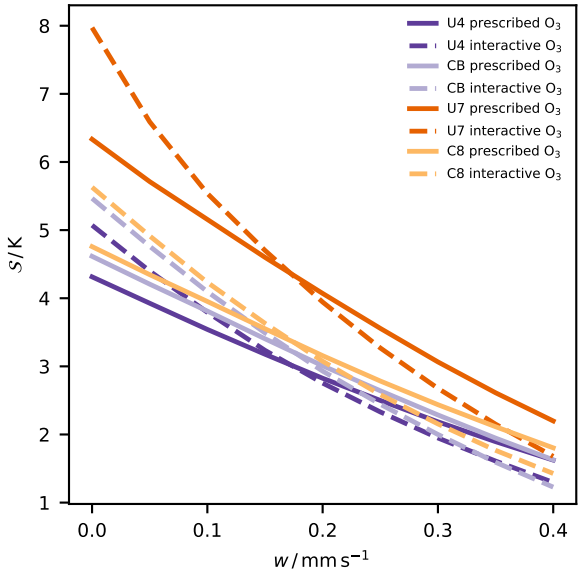

FIG. 6. Tropical equilibrium climate sensitivity $\mathcal{S}$ as a function of w. Continuous line: prescribed O_3. Dashed line: Cariolle O_3. Different colors indicate the different RH profile: U4 dark purple, CB light purple, U7 dark orange, and C8 light orange.

5. The tropical energy export and feedbacks in GCMs

An analysis of CMIP models (not shown) confirms that models with a larger ECS, i.e., models which produce larger surface warming, in general simulate a stronger increase of the tropical upwelling. In the RCE experiments, we control the upwelling speed and show that $\mathcal{S}$ decreases with increasing upwelling speed. Therefore, we conclude that for a given GCM, if there was no increase in upwelling with surface warming, the tropical equilibrium climate sensitivity would be larger than with the actual increase in the tropical upwelling.

In the RCE model, the change in the tropical energy export is the main factor for the reduced tropical equilibrium climate sensitivity. Here, we test if there is a similar dependence of the tropical energy export N_e on the upwelling change in an ensemble of CMIP5 and CMIP6 models. These GCMs are usually not run up to equilibrium in the abrupt-4xCO2 experiments. Hence, we linearly regress the tropical (from 25°S to 25°N) on the global TOA net

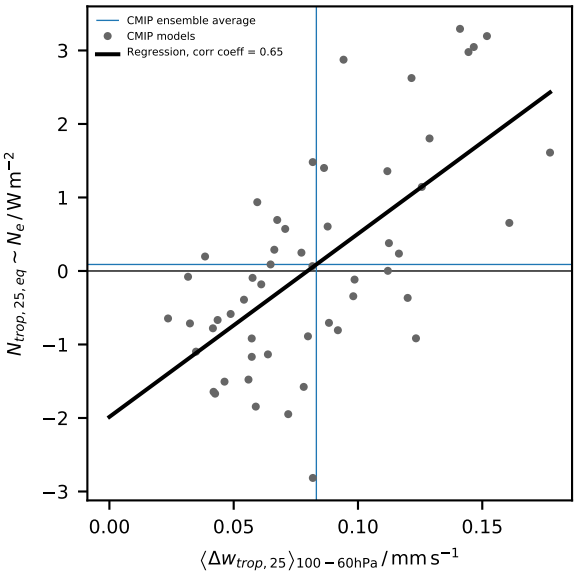

FIG. 7. Tropical TOA net radiative flux in relation to tropical upwelling speed changes in GCMs. The y-axis shows N_e calculated in the tropical band from 25°S to 25°N compared to the change in upwelling speed averaged in the range 100 hPa to 60 hPa. The blue lines show the ensemble mean values.

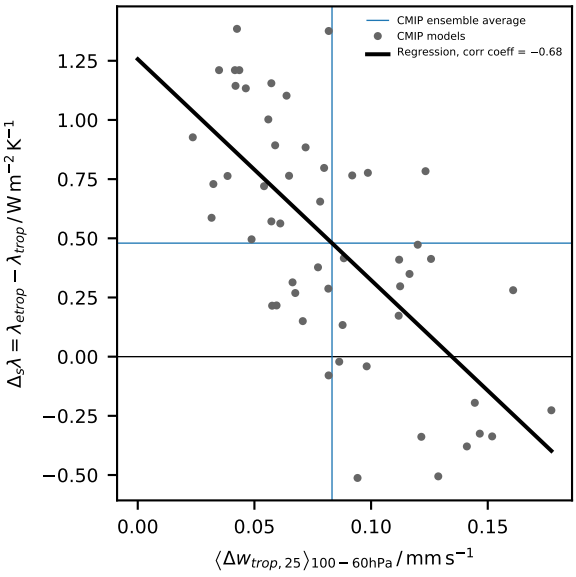

FIG. 8. Difference of tropical and extratropical radiative feedbacks in relation to the change in upwelling speed in GCMs. The blue lines show the ensemble mean values. The black line is the linear regression that represents the relationship.

radiative flux for each GCM. The y-intercepts provide estimates of the change in the tropical energy export N_e. Figure 7 shows these estimates of N_e versus the upwelling speed change averaged over 100 hPa to 60 hPa. The linear regression ($r = 0.65$) of the change in the upwelling speed vs. the tropical energy export shows a relationship which is similar in several ways to the one found with `konrad` (Figure 2): (a) with increasing upwelling change, the change in the tropical energy export increases; (b) for very small upwelling change, the tropical energy export is smaller than in the pre-industrial control; (c) if it is sufficiently large, there is a larger export than in the pre-industrial control; and (d) there is an upwelling speed change that provides no change in the tropical energy export.

As mentioned before, the change in the tropical energy export strongly influences $\mathcal{S}$ in `konrad`. How does it affect the global climate sensitivity in GCMs? An increase in tropical upwelling needs to be accompanied by an increased extratropical stratospheric downwelling, causing an adiabatic warming. This warming affects the extratropical radiative flux, potentially leading to a change in the global net radiative feedback. More precisely, we expect more outgoing long-wave radiation for a larger increase in the tropical energy export, resulting in a stronger (i.e. more negative) extratropical net radiative feedback. We calculate the difference $\Delta_s\lambda$ between the extratropical (λ_{etrop}) and the tropical (λ_{trop}) net radiative feedbacks to evaluate this change. The difference is computed as follows

$$\Delta_s\lambda = \frac{\lambda - \lambda_{\text{trop}}}{1 - \alpha}, \tag{5}$$

where the individual radiative feedback parameters are calculated from the corresponding NT-diagrams, and α is the surface fraction of the used tropical band ($\alpha \approx 0.28$). Figure 8 shows that this meridional contrast in the radiative feedback depends on the tropical upwelling speed change ($r = 0.68$). For smaller upwelling changes, the extratropical feedback is weaker (less negative), whereas larger changes provide an extratropical feedback comparable to or stronger than the tropical feedback. Thus, if the tropical stratospheric upwelling would not increase in a GCM, the extratropical stratospheric warming would be smaller, the extratropical and global radiative feedbacks weaker, and the global ECS larger.

6. Summary of the results

a. `konrad` experiments

Changes in the tropical energy export produced by a changing tropical stratospheric upwelling affect the tropical equilibrium climate sensitivity, regardless of the exact mechanism of the upwelling change. Due to this effect, the tropics can equilibrate at a non-zero TOA net radiative flux change. In the context of an RCE model of the tropics, the dominant effect of the increased upwelling is

an increased energy export which is represented as a reduction of the effective forcing. However, the increase in upwelling also affects the radiative part of the forcing and the net radiative feedback. The radiative forcing increases for increasing upwelling due to the adjustment of the stratospheric temperature which reduces the OLR and dominates a counteracting increase due to the adjustment of the water vapor to the reduced temperature. The way in which the change in upwelling is applied in numerical experiments, instantaneously or gradually, only affects the share between the forcing and feedback contributions (Figures 2 and 4), but not the resulting tropical equilibrium climate sensitivity. A change in the tropical stratospheric upwelling due to increasing CO_2 is better represented by the experiments in which the upwelling is increased gradually following equation (2). In this case, the increasing adiabatic cooling in the TTL relates to the surface warming, weakening the lapse-rate feedback. This weakened lapse-rate feedback comes with a corresponding reduction in the effective radiative forcing (Figure 5). Interactive O_3 strengthens the net radiative feedback by producing a weaker water-vapor feedback. This weaker water-vapor feedback overcompensates the weaker lapse-rate feedback introduced by the upwelling, greatly strengthening the net radiative feedback and its share (Figure 4) in the reduction of the tropical equilibrium climate sensitivity.

The case of the instantaneous change in the upwelling speed may be considered more representative of the upwelling change caused by volcanic stratospheric aerosol (e.g., Niemeier et al. 2011), although the lapse rate change in the TTL would be opposite to our experiment. In those experiments, the net radiative feedback barely changes with the upwelling speed (Figure 2). The adiabatic cooling in the TTL is applied instantaneously, affecting the stratospheric adjustment, slightly increasing the effective radiative forcing with increasing upwelling (Figure 1) as described above. Interactive O_3 has a similar effect in the instantaneous case as in the gradual case: it strengthens the net radiative feedback, but does not change appreciably the feedback contribution to the reduction of the tropical equilibrium climate sensitivity.

b. The contributions of a realistic change in upwelling speed

In the analysis, we show that an increase of the upwelling modifies the forcing and feedback contributions to the reduction of $\mathcal{S}$. Here, we estimate the magnitude of these effects for a reasonable assumption of an upwelling increase. Observations indicate that the upwelling speed increases at a rate of $\sim 0.005\,\mathrm{mm\,s^{-1}}$ per decade (Fu et al. 2019). Assuming that this rate is sustained during a 200-year CO_2-doubling experiment in a GCM, the total increase would be of $\sim 0.1\,\mathrm{mm\,s^{-1}}$. Therefore, we derive estimates from the experiments for an increase from $w^c = 0.2\,\mathrm{mm\,s^{-1}}$ to $w_e \approx 0.3\,\mathrm{mm\,s^{-1}}$. Assuming that the O_3 response to quadrupling CO_2 would be approximately twice that from a doubling of CO_2 the comparison between our `2xCO2` experiments and the `abrupt-4xCO2` experiments from GCMs with interactive chemistry in Table 3 indicates that `konrad` produces a reasonable O_3 response to an upwelling change of $\sim 0.1\,\mathrm{mm\,s^{-1}}$.

Table 4 shows the relative changes in tropical equilibrium climate sensitivity ($\mathcal{S}$), effective forcing (F), and net radiative feedback (λ) arising from a $\sim 0.1\,\mathrm{mm\,s^{-1}}$ increase in upwelling. Without interactive O_3, the increase in upwelling reduces $\mathcal{S}$ by 24% . The atmospheric composition feedback from O_3 increases this reduction to 29%. This shows that the main contribution comes from the direct, adiabatic effect of the upwelling change. In the case of prescribed O_3 and a gradual upwelling change, the contribution of the forcing to the reduction of $\mathcal{S}$ is of 126% while the contribution of λ is negative, -26%, due to the reduction of the lapse rate feedback. Adding interactive O_3 strengthens the net radiative feedback, reducing the contribution of F to 75% and increasing that of λ to 25%.

c. GCMs

In GCMs, a higher equilibrium climate sensitivity would, in general, entail a stronger increase of the upwelling speed in experiments with CO_2 increase compared to the pre-industrial control. This is not in contradiction with `konrad` results. We hypothesize that the upwelling change provides a negative feedback to the warming and without increasing upwelling the spread of the model's ECSs would be even larger. This is supported by the result that GCMs show a similar relationship between the changes in the tropical energy export and the upwelling speed change as in `konrad` (Figure 7). While tropical adiabatic cooling and extratropical warming could result in a globally zero effect, our analysis of the CMIP ensemble of GCMs also shows that the change in the tropical energy export leads to a change in the extratropical feedback: the stronger the upwelling change, the stronger the extratropical feedback is in relation to the tropical one (Figure 8). The extratropical stratospheric warming increases the lapse rate feedback, and thereby the OLR in this region, which leads very likely to a lower global equilibrium climate sensitivity in relation to a situation without tropical stratospheric upwelling change.

7. Discussion and conclusions

By introducing the dynamical cooling of the tropical BDC upwelling via the term (1), we enable to study the influence of the stratospheric upwelling changes on the tropical ECS in an clear-sky RCE framework. However, since the cooling term can be seen as an export of energy to the extratropics, the interpretation of the results for

O_3	w change	w / mm s^{-1}	$\Delta_r\mathcal{S}$ / 1	$\Delta_r F$ / 1	$\Delta_r\lambda$ / 1	$\Delta_{r,F}\mathcal{S}$ / 1	$\Delta_{r,\lambda}\mathcal{S}$ / 1
prescribed	gradual	0.307	−0.24	−0.30	−0.08	1.26	−0.26
	instantaneous			−0.23	0.02	0.94	0.06
interactive	gradual	0.298	−0.29	−0.22	0.10	0.75	0.25
	instantaneous			−0.27	0.04	0.91	0.09

TABLE 4. Relative changes in $\mathcal{S}$, F and λ due to a ~0.1 mm s^{-1} increase in upwelling (columns four to six). The first column indicates if the O_3 was prescribed or calculated interactively with the Cariolle scheme, the second column if the experiment used a gradual or instantaneous change of the upwelling speed to the value given in the third column. Last two columns: Contributions of F and λ, respectively, to the change of $\mathcal{S}$.

the global ECS is not straightforward. Before coming to this, we will discuss a few assumptions made in the RCE framework.

In particular, it does not include a representation of the drivers of the circulation changes. More baroclinicity due to changes in the meridional temperature gradient tends to increase wave activity and subsequently the influence of wave drag on the stratospheric angular momentum balance and tropical upwelling (Eichelberger and Hartmann 2005; Chen and Sun 2011; Butchart 2014). In our simplified model, we arbitrarily increase the upwelling speed in a somewhat arbitrarily chosen altitude range, leading to an arbitrary increase in the tropical energy export. However, comparison with observations indicates that our assumptions of an upwelling increase for a given CO_2 forcing and its effect on the vertical distribution of O_3 are in the possible range.

Another issue in our simulations, as in the 1D-RCE approach in general, is the parameterized convection. Deep convection would change due to the changing stability in the upper troposphere with faster upwelling (Figure 3), suggesting a possible interaction of overshooting convection with the effects of upwelling (see, e.g., Folkins 2002; Holloway and Neelin 2007; Dauhut and Hohenegger 2022). This interaction is relevant because it can modify temperature and humidity in the upper troposphere and influence the change in the tropical energy export and the tropical radiative feedback mechanisms.

A further issue is the clear-sky approach. As we can see from the GCM results, the relationship between BDC acceleration and tropical energy export exists as in `konrad` simulations: they agree qualitatively (Figure 7). However, there is a quantitative difference and substantial variance that is not explained by the change in circulation. This also applies for the difference in the tropical and extratropical radiative feedbacks (Figure 8). Clouds, in addition to convection and tropospheric circulation changes, may contribute to this. The relation of clouds and convection makes the connection even more relevant. This is a strong reason to study how clouds fit into the relationship uncovered in our study.

Despite these limitations, we consider the detected relationship between the stratospheric upwelling and tropical climate sensitivity as robust. This relationship has not received much attention, yet, probably because BDC changes are represented in GCMs. An increase in the tropical stratospheric upwelling alone strongly reduces the tropical equilibrium climate sensitivity by increasing the energy export from the tropics to the extratropics. Since, in our framework, this export is represented as a forcing, the largest contribution to the reduction of the tropical climate sensitivity is due to a forcing change. The contribution of a change in the radiative feedback is in general small.

In our experiments, more than 70% of the reduction of the tropical climate sensitivity by increased upwelling are caused by the direct effect of adiabatic cooling. The much discussed effect from the upward shift of the O_3 profile contributes less than 30%. It is interesting to note that despite both mechanisms leading to a cooling of the TTL they affect radiation very differently. Because of a strong cooling effect at the cold point tropopause, the O_3 shift strongly reduces water vapor and its greenhouse effect, and hence increases OLR. The dominant radiative consequence of the adiabatic cooling is a reduction of OLR through the lapse rate effect.

Another important finding is that the specific choice of upper-tropospheric RH does not alter the relationship between upwelling and tropical climate sensitivity. However, the relationship is shifted to higher sensitivity for large middle-tropospheric RH values by closing the atmospheric window, e.g., the U7 profile (Bourdin et al. 2021): a large middle-tropospheric RH leads to higher specific humidity in that region. Higher specific humidity means weaker planetary long-wave emissivity, thereby weakening the effect of the tropical energy export. Remarkable is that such climates can become more stable with greater upwelling speeds. Therefore, some humid palæoclimates might be stabilized by strong changes in circulation.

Our experiments cannot be conclusive concerning the effect of upwelling on global ECS. However, the analysis of CMIP GCMs shows that models with a stronger upwelling change, in general also simulate a stronger increase of the energy export to the extratropics, similar as simulated by our RCE experiments. Moreover, the warming in the extratropical stratosphere resulting from this export likely affects surface temperature less than the cooling in the

tropics because it should enhance the negative lapse rate feedback but much less affect the greenhouse effect of water vapor than the cooling in the tropics. This is supported by our analysis showing that the difference of extratropical and tropical radiative feedbacks in GCMs in general decreases more strongly (gets more negative) for models with larger upwelling increases. It is hence very likely that the increase of BDC upwelling provides a global negative radiative feedback not only through the upward shift of the O_3 profile but also, and possibly more strongly, through its adiabatic cooling. Dedicated GCM experiments will be needed to better quantify this effect.

Acknowledgments. We thank Sally Dacie, Clarissa Kroll, Jiawei Bao, Hans Segura, Geet George, and Moritz Günther, for useful comments on an earlier draft of the manuscript, and for discussing the ideas giving life to this study. The Max-Planck Gesellschaft (MPG) and the Bundesministerium für Bildung und Forschung (BMBF) through the ROMIC2-SOCTOC project support our research. We use computational resources from the Deutsches Klimarechenzentrum (DKRZ).

Data availability statement. All the data for reproducing this study is available in Zenodo repositories 10.5281/zenodo.6482543 (`konrad` results) and 10.5281/zenodo.6482451 (post-processed CMIP data).

References

Abalos, M., B. Legras, F. Ploeger, and W. J. Randel, 2015: Evaluating the advective Brewer-Dobson circulation in three reanalyses for the period 1979–2012. *J. Geophys. Res. Atmos.*, **120 (15)**, 7534–7554, https://doi.org/10.1002/2015JD023182.

Bao, Jiawei and Stevens, Bjorn and Kluft, Lukas and Jiménez-de-la-Cuesta, Diego, 2021: Changes in the Tropical Lapse Rate due to Entrainment and Their Impact on Climate Sensitivity. *Geophys. Res. Lett.*, **48 (18)**, e2021GL094 969, https://doi.org/10.1029/2021GL094969.

Birner, T., and E. J. Charlesworth, 2017: On the relative importance of radiative and dynamical heating for tropical tropopause temperatures. *J. Geophys. Res. Atmos.*, **122 (13)**, 6782–6797, https://doi.org/10.1002/2016JD026445.

Bourdin, S., L. Kluft, and B. Stevens, 2021: Dependence of Climate Sensitivity on the Given Distribution of Relative Humidity. *Geophys. Res. Lett.*, **48 (8)**, e2021GL092 462, https://doi.org/10.1029/2021GL092462.

Brewer, A. W., 1949: Evidence for a world circulation provided by the measurements of helium and water vapor distribution in the stratosphere. *Quart. J. Roy. Meteor. Soc.*, **75 (326)**, 351–363, https://doi.org/10.1002/qj.49707532603.

Butchart, N., 2014: The Brewer-Dobson circulation. *Rev. Geophys.*, **52 (2)**, 157–184, https://doi.org/10.1002/2013RG000448.

Cariolle, D., and H. Teyssèdre, 2007: A revised linear ozone photochemistry parameterization for use in transport and general circulation models: multi-annual simulations. *Atmos. Chem. Phys.*, **7 (9)**, 2183–2196, https://doi.org/10.5194/acp-7-2183-2007.

Chen, G., and L. Sun, 2011: Mechanisms of the Tropical Upwelling Branch of the Brewer–Dobson Circulation: The Role of Extratropical Waves. *J. Atmos. Sci.*, **68 (12)**, 2878–2892, https://doi.org/10.1175/JAS-D-11-044.1.

Chiodo, G., and L. M. Polvani, 2019: The Response of the Ozone Layer to Quadrupled CO2 Concentrations: Implications for Climate. *J. Climate*, **32 (22)**, 7629–7642, https://doi.org/10.1175/JCLI-D-19-0086.1.

Dacie, S., and Coauthors, 2019: A 1D RCE Study of Factors Affecting the Tropical Tropopause Layer and Surface Climate. *J. Climate*, **32 (20)**, 6769–6782, https://doi.org/10.1175/JCLI-D-18-0778.1.

Dauhut, T., and C. Hohenegger, 2022: The Contribution of Convection to the Stratospheric Water Vapor: The First Budget Using a Global Storm-Resolving Model. *J. Geophys. Res. Atmos.*, **127 (5)**, e2021JD036 295, https://doi.org/10.1029/2021JD036295.

Dietmüller, S., M. Ponater, and R. Sausen, 2014: Interactive ozone induces a negative feedback in CO2-driven climate change simulations. *J. Geophys. Res. Atmos.*, **119 (4)**, 1796–1805, https://doi.org/10.1002/2013JD020575.

Dobson, G. M. B., 1956: Origin and distribution of polyatomic molecules in the atmosphere. *Proc. Roy. Soc.*, **236 (1205)**, 187–193, https://doi.org/10.1098/rspa.1956.0127.

Eichelberger, S. J., and D. L. Hartmann, 2005: Changes in the strength of the Brewer-Dobson circulation in a simple AGCM. *Geophys. Res. Lett.*, **32 (15)**, L15 807, https://doi.org/10.1029/2005GL022924.

Eyring, V., S. Bony, G. A. Meehl, C. A. Senior, B. Stevens, R. J. Stouffer, and K. E. Taylor, 2016: Overview of the Coupled Model Intercomparison Project Phase 6 (CMIP6) experimental design and organization. *Geosci. Model Dev.*, **9 (5)**, 1937–1958, https://doi.org/10.5194/gmd-9-1937-2016.

Folkins, I., 2002: Origin of Lapse Rate Changes in the Upper Tropical Troposphere. *J. Atmos. Sci.*, **59 (5)**, 992–1005, https://doi.org/10.1175/1520-0469(2002)059<0992:OOLRCI>2.0.CO;2.

Fu, Q., S. Solomon, H. A. Pahlavan, and P. Lin, 2019: Observed changes in Brewer–Dobson circulation for 1980–2018. *Environ. Res. Lett.*, **14 (11)**, 114 026, https://doi.org/10.1088/1748-9326/ab4de7.

Gregory, J., and Coauthors, 2004: A new method for diagnosing radiative forcing and climate sensitivity. *Geophys. Res. Lett.*, **31 (3)**, L03 205, https://doi.org/10.1029/2003GL018747.

Holloway, C. E., and J. D. Neelin, 2007: The Convective Cold Top and Quasi Equilibrium. *J. Atmos. Sci.*, **64 (5)**, 1467–1487, https://doi.org/10.1175/JAS3907.1.

Kluft, L., S. Dacie, S. A. Buehler, H. Schmidt, and B. Stevens, 2019: Re-Examining the First Climate Models: Climate Sensitivity of a Modern Radiative–Convective Equilibrium Model. *J. Climate*, **32 (23)**, 8111–8125, https://doi.org/10.1175/JCLI-D-18-0774.1.

Manabe, S., and R. F. Strickler, 1964: Thermal Equilibrium of the Atmosphere with a Convective Adjustment. *J. Atmos. Sci.*, **21 (4)**, 361–385, https://doi.org/10.1175/1520-0469(1964)021<0361:TEOTAW>2.0.CO;2.

Manabe, S., and R. T. Wetherald, 1967: Thermal Equilibrium of the Atmosphere with a Given Distribution of Relative Humidity. *J. Atmos. Sci.*, **24 (3)**, 241–259, https://doi.org/10.1175/1520-0469(1967)024<0241:TEOTAW>2.0.CO;2.

Marsh, D. R., J.-F. Lamarque, A. J. Conley, and L. M. Polvani, 2016: Stratospheric ozone chemistry feedbacks are not critical for the determination of climate sensitivity in CESM1 (WACCM). *Geophys. Res. Lett.*, **43 (8)**, 3928–3934, https://doi.org/10.1002/2016GL068344.

Meraner, K., S. Rast, and H. Schmidt, 2020: How Useful Is a Linear Ozone Parameterization for Global Climate Modeling? *J. Adv. Model. Earth Syst.*, **12 (4)**, e2019MS002 003, https://doi.org/10.1029/2019MS002003.

Muthers, S., and Coauthors, 2014: The coupled atmosphere-chemistry-ocean model SOCOL-MPIOM. *Geosci. Model Dev.*, **7 (5)**, 2157–2179, https://doi.org/10.5194/gmd-7-2157-2014.

Niemeier, U., H. Schmidt, and C. Timmreck, 2011: The dependency of geoengineered sulfate aerosol on the emission strategy. *Atmospheric Science Letters*, **12 (2)**, 189–194.

Nowack, P. J., N. L. Abraham, P. Braesicke, and J. A. Pyle, 2018: The Impact of Stratospheric Ozone Feedbacks on Climate Sensitivity Estimates. *J. Geophys. Res. Atmos.*, **123 (9)**, 4630–4641, https://doi.org/10.1002/2017JD027943.

Nowack, P. J., N. L. Abraham, A. C. Maycock, P. Braesicke, J. M. Gregory, M. M. Joshi, A. Osprey, and J. A. Pyle, 2015: A large ozone-circulation feedback and its implications for global warming assessments. *Nat. Clim. Change*, **5 (1)**, 41–45, https://doi.org/10.1038/nclimate2451.

Ramanathan, V., and J. Coakley, 1978: Climate Modeling Through Radiative-Convective Models. *Rev. Geophys.*, **16 (4)**, 465–489, https://doi.org/10.1029/RG016i004p00465.

Taylor, K. E., R. J. Stouffer, and G. A. Meehl, 2012: An Overview of CMIP5 and the Experiment Design. *Bull. Amer. Meteor. Soc.*, **93 (4)**, 485–498, https://doi.org/10.1175/BAMS-D-11-00094.1.

Yoshida, K., R. Mizuta, and O. Arakawa, 2018: Intermodel Differences in Upwelling in the Tropical Tropopause Layer Among CMIP5 Models. *J. Geophys. Res. Atmos.*, **123 (24)**, 13 658–13 675, https://doi.org/10.1029/2018JD029044.